Proc. 2nd Japan-China Joint Workshop on Positron Science
JJAP Conf. Proc. **2** (2014) 011209

Study of Reversibility of Self-assembly in Saponite Layered Nanoparticles

Kazuomi Numata and Kiminori Sato*

Department of Environmental Sciences, Tokyo Gakugei University, 4–1–1 Koganei, Tokyo 184–8501, Japan.

E-mail: sato-k@u-gakugei.ac.jp

(Received Jun. 30, 2014)

The reversible process of self-assembly involving the rheological motion of 2-dimensional nanosheets with the aid of water molecules was studied for saponite inorganic layered nanoparticles by dilatometry and positronium lifetime spectroscopy. The two nanosheet insertion type local molecular structure, dominant in the dehydrated state, was not fully reproducible upon dehydration for the self-assembled sample. The two nanosheet insertion type local structure could thus disappear when saponite goes through self-assembly several times. It was furthermore found that a local structure with a void size slightly larger than that in the two nanosheet insertion type structure exists before self-assembly. This structure, presumably due to curved nanosheets, is metastable and gradually disappears during self-assembly.

1. Introduction

2-dimensional (2D) nanosheets in inorganic layered nanoparticles spontaneously agglomerate with well-defined local structures through their mutual interactions with the aid of H_2O molecules [1, 2]. This agglomeration process is called self-assembly of 2D nanosheets. Based on our recent findings by positronium (Ps) annihilation spectroscopy together with molecular dynamics (MD) simulations, the following rheological mechanism has been proposed for saponite layered nanoparticles [3]. Before self-assembly saponite nanoparticles possess two kinds of local molecular structures, where one and two nanosheets are inserted into the interlayer spaces forming voids with sizes of ∼0.3 nm and ∼0.9 nm, respectively. H_2O molecules trigger off the self-assembly of saponite nanoparticles. H_2O molecules adsorbed on the Na^+ cations in the interlayer spaces act as a lubricant, causing the rheological motion of nanosheets parallel to the layer direction. One of two nanosheets inserted into the interlayer spaces are thus released away. The local molecular structures with larger voids are gradually altered to those with smaller voids which become dominant for the self-assembled saponite nanoparticles.

It has been found that the above-mentioned two nanosheet insertion type local molecular structure, referred to as type B, appearing during self-assembly is associated with a number of global environmental issues [4–6]. For example, the characteristic local structures as a nanosheet edge and a wedge-shaped frayed part available in the voids of type B are responsible for site specific Cs adsorption [4, 5]. Pore fluid in this local structure has been suggested to be related to earthquake slip weakening in plate-boundary faults [6]. In the present study, the reversibility of self-assembly involving the rheological motion of 2D nanosheets with the aid of H_2O molecules was studied for saponite inorganic layered nanoparticles by means of X-ray diffraction (XRD), dilatometry (DLT), and Ps annihilation spectroscopy. We focus particularly on the reversibility of the type B structure upon dehydration of the self-assembled state. The gradual disappearance of the metastable local structure with self-assembly is also explored.

2. Experiments

Synthetic Na-type saponite samples with a particle size of approximately 45 nm in diameter (54.71 % SO_2, 5.02 % Al_2O_3, 0.03 % Fe_2O_3, 30.74 % MgO, 2.15 % Na_2O, 0.07 % CaO, 0.67 % SO_3, 6.64 % H_2O) produced by Kunimine Industries Co. Ltd., Japan were employed in this study. XRD measurements were conducted for the following three samples: as-received powder, a pellet prepared by uniaxial compaction, and powder after baking at 423 K for 12 h in vacuum of 10^{-3} Pa.

Length-change measurements were performed for the uniaxially compacted pellet samples with a high-precision differential-type dilatometer (TD5020SA, Bruker AXS) equipped with a closed-water-cycling system. The dilatometer system is fully cooled, keeping a constant temperature with high thermal stability and thus preventing temperature overshoot and runaway, which enables us to perform long-term measurements [7]. The pellet sample was initially dehydrated at 423 K for 12 h in a vacuum of 10^{-3} Pa, and was then exposed to a humidity of ~35 % at a temperature of ~300 K, where time-dependent data were obtained (1st measurement run). After completing the length change, the sample was dehydrated under the same baking condition in vacuum, and was exposed again to the same humidity and temperature, where time-dependent data were again obtained (2nd measurement run).

Ps lifetime spectroscopy was conducted to characterize the angstrom-scale open spaces. A fraction of energetic positrons injected into samples forms the positron-electron bound state, Ps. Singlet *para*-Ps (*p*-Ps) with the spins of the positron and electron antiparallel and triplet *ortho*-Ps (*o*-Ps) with parallel spins are formed at a ratio of 1 : 3. Hence, three possible positron states: *p*-Ps, *o*-Ps, and free positrons exist in the samples. The annihilation of *p*-Ps results in the emission of two γ-ray photons of energy 511 keV with a lifetime of ~125 ps. Free positrons are trapped by negatively charged parts, such as polar elements, and annihilate into two photons with a lifetime of ~450 ps. The positron in *o*-Ps undergoes two-photon annihilation with one of the electrons bound to surrounding molecules with a lifetime of a few ns after localization in angstrom-scale pores. The process is known as *o*-Ps pick-off annihilation and the lifetime of this process $\tau_{o\text{-Ps}}$ can be related to the open size radius R through the Tao-Eldrup model [8, 9]:

$$\tau_{o\text{-Ps}} = 0.5\left[1 - \frac{R}{R_0} + \frac{1}{2\pi}\sin\left(\frac{2\pi R}{R_0}\right)\right]^{-1} \tag{1}$$

where $R_0 = R + \Delta R$, and $\Delta R = 0.166$ nm is the thickness of homogeneous electron layer in which the positron in *o*-Ps annihilates.

The positron source (^{22}Na) was sealed in a thin foil of Kapton and was buried in the sample powder, which was prepared with the same conditions as described above for the DLT measurements of the pellet sample. The time-dependent data of the 1st and 2nd measurement runs were obtained every 45 min under the same conditions as that of DLT. The validity of our lifetime measurements and data analysis was confirmed with certified reference materials (NMIJ CRM 5601-a and 5602-a) provided by the National Metrology Institute of Japan, National Institute of Advanced Industrial Science and Technology (AIST) [10, 11]. Positron lifetime spectra were numerically analyzed using the POSITRONFIT code [12].

3. Results and discussions

Figure 1 shows XRD patterns observed for samples with powder (bottom), pellet prepared by uniaxial compaction (middle), and powder after baking in vacuum (top). The diffraction pattern of the powder sample is of typical 2 : 1 layered structure of saponite nanoparticles characterized by (020), (004), (130), (310), and (060) peaks. This demonstrates that the 2D nanosheets are periodically ordered. No significant narrowing and peak shift are however observed in the diffraction patterns of the pellet (middle) and vacuum baked samples (top). It is expected that narrowing of diffraction peaks should

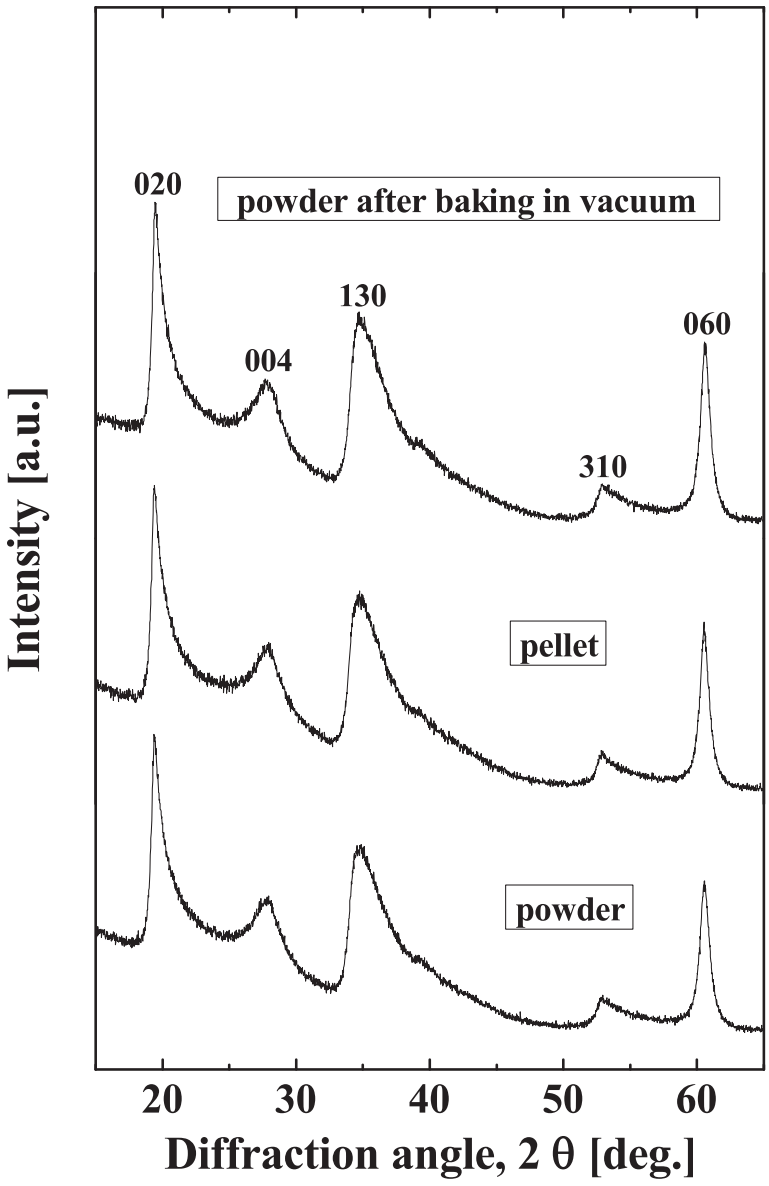

Fig. 1. XRD patterns observed for conventional powder (bottom), pellet prepared by uniaxial compaction (middle), and powder after baking at 423 K for 12 h in vacuum of 10^{-3} Pa (top).

occur for the pellet sample because 2D nanosheets are stacked with a well-ordered state. On the other hand, a peak shift is expected for the sample after baking in vacuum because the interlayer space shrinks due to removal of H_2O molecules by dehydration. The lack of significant narrowing and peak shift imply the difficulty of probing the variation of basal spacing caused by ordering of 2D nanosheets as well as dehydration, which are responsible for self-assembly. It was not possible to observe the reversible process of local molecular structure change during self-assembly by XRD.

Figure 2 shows length changes as a function of exposure time obtained in the 1st and 2nd measurement runs. The length change increases with increasing the exposure time both in the 1st and 2nd measurement runs. As mentioned above, the present saponite nanoparticles were uniaxially compacted forming a pellet for the length-change measurements with DLT, in which the 2D nanosheets

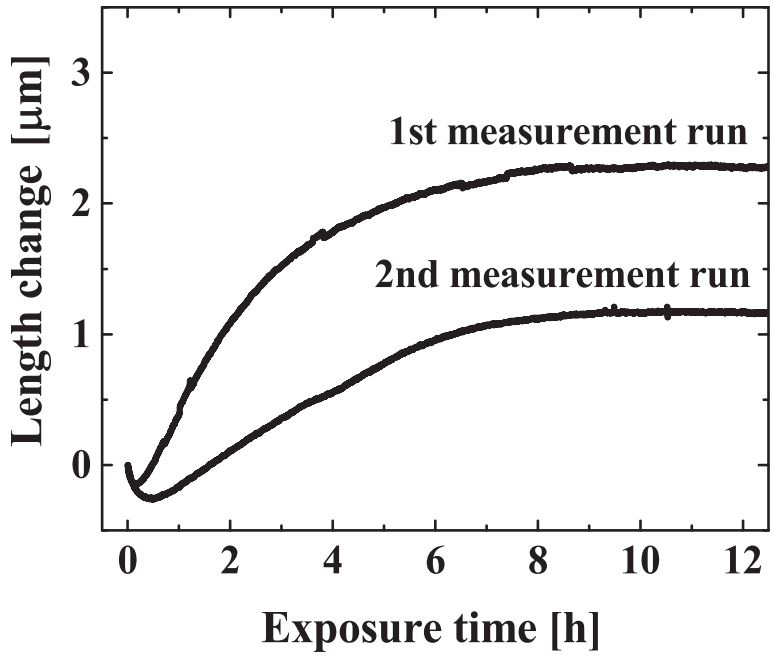

Fig. 2. Length changes of saponite layered nanoparticles as a function of exposure time obtained in the 1st and 2nd measurement runs. See text as for the description of the measurement run conditions.

are well ordered perpendicularly to the compaction direction. H_2O adsorption in the interlayer spaces locally expands the basal spacing as has been assessed by XRD under controlled relative humidity conditions [13]. The increase of macroscopic length change with exposure time is thus caused by an expansion of basal spacing.

It is seen from Fig. 2 that the increases in length is largely suppressed in the 2nd measurement run. Our previous Ps lifetime spectroscopy results with MD simulation has revealed that the two-nanosheet insertion type local molecular structure, so-called type B, is dominant before self-assembly, whereas the one-nanosheet insertion type local molecular structure, so-called type A, is dominant for the self-assembled sample [3]. Expansion of the basal spacing in type A is smaller than that of type B, because one nanosheet is inserted into the interlayer space. The suppression of macroscopic length change in the 2nd measurement run is thus a consequence of less expansion of basal spacing in the ordered state with stacked 2D nanosheets, in which type A is initially dominant, owing to sufficient self-assembly during the 1st measurement run. Of importance here is that the type B local molecular structure is not fully reproducible after the 1st self-assembly even though the sample was dehydrated again before the 2nd measurement run.

The irreversible nature of the type B structure can also be inferred from the time-dependent *o*-Ps lifetime τ_4 and corresponding relative intensity I_4 in the 1st and 2nd measurement runs shown in Fig. 3. In the 1st measurement run, both *o*-Ps lifetime τ_4 and relative intensity I_4 decrease with exposure time up to 240 h. This is much longer than those of the hydration processes observed by solid-state nuclear magnetic resonance (NMR) spectroscopy and the gravimetric measurements, going only up to 8 h, as detailed in our earlier works [2, 3]. It is thus expected that the decrease in the *o*-Ps lifetime τ_4 and relative intensity I_4 is caused by the release of one nanosheet in type B changing to type A due to self-assembly. For the 2nd measurement run the relative intensity I_4 at an exposure time of 0 h is significantly lower that of the 1st measurement run, signifying that type B is not fully reproducible, consistent with the results of DLT experiments. In addition, the *o*-Ps lifetime τ_4 is lower

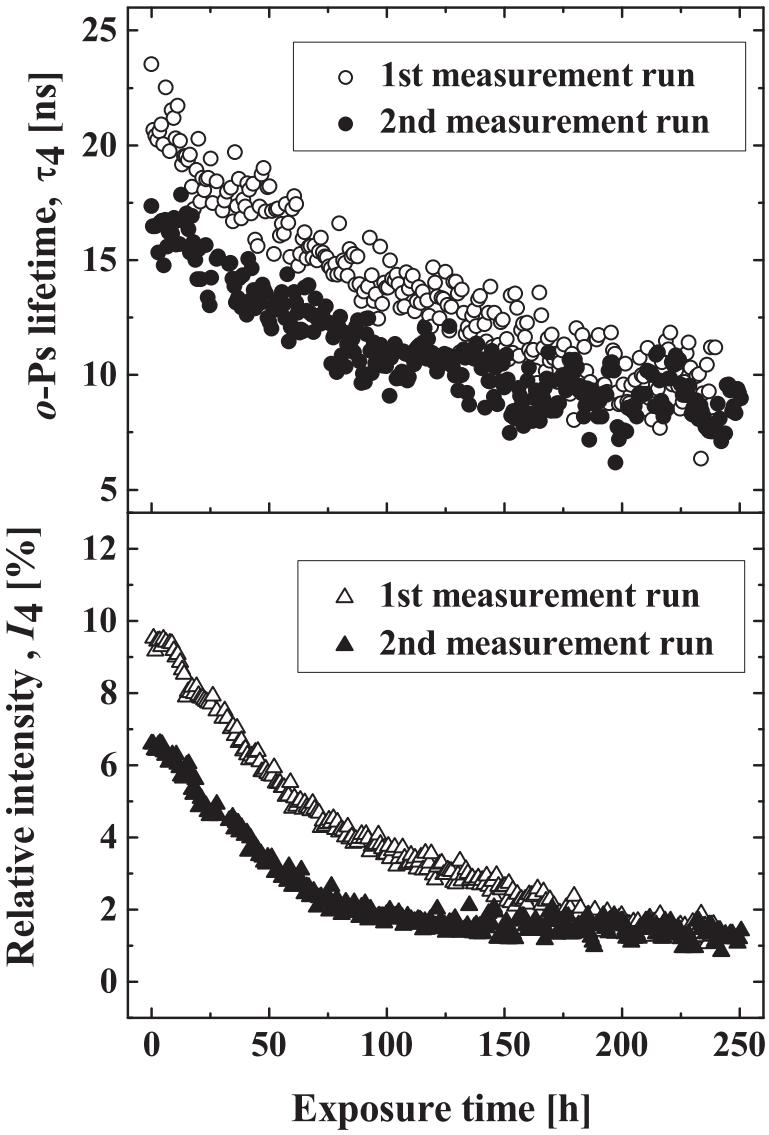

Fig. 3. *o*-Ps lifetimes τ_4 and corresponding relative intensities I_4 as a function of exposure time in the 1st (open symbols) and 2nd (solid symbols) measurement runs.

than that of the 1st measurement run at an exposure time of 0 h. This gives additional information on the local molecular structure after the 2nd dehydration, which possesses voids slightly smaller than that in type B. In other words, the local structure with the void slightly larger than that in the type B exits together with type B after the 1st dehydration.

In the light of the fact that the relative intensity I_4 in the 2nd measurement run coincides with that of 1st measurement run around 200 h, the local molecular structure identified above would be metastable. MD simulations have speculated that the stationary structure of 2D nanosheets has a curved shape under external stress [14]. Such a curved nanosheet existing before self-assembly could form a local structure with voids slightly larger than that in type B. The curved nanosheets become flat slowly together with the rheological motion of nanosheets parallel to the layer direction, by which the above-mentioned local structure disappears. On the one hand, the type B local structure dominantly existing before self-assembly is found not to be fully reproduced by dehydration after self-assembly.

Presumably, type B would completely disappear even immediately after dehydration if the sample goes through the process of self-assembly several times.

4. Conclusion

In order to study the reversibility of self-assembly involving the rheological motion of 2D nanosheets with the aid of water molecules in saponite layered nanoparticles, well self-assembled samples were dehydrated and then exposed to humidity for re-self-assembly. Molecular process of the 2D nanosheets was investigated by XRD, DLT and Ps lifetime spectroscopy. XRD studies focusing on the basal spacing were found to be unsuitable for probing the reversible process of local molecular structure with self-assembly and dehydration. DLT and Ps lifetime spectroscopy successfully demonstrated that the two nanosheet insertion type local structure, which is dominant before self-assembly, was not fully reproduced upon dehydration for the self-assembled sample. This local structure could thus gradually disappear with increasing numbers of self-assemblies. Furthermore, it was found by Ps lifetime spectroscopy that a local structure with voids slightly larger than that in two-nanosheet insertion type structure exists before self-assembly. This structure, presumably due to curved nanosheets, is metastable and gradually disappears during self-assembly.

Acknowledgment

The authors are indebted to K. Fujimoto (Tokyo Gakugei University) and K. Kawamura (Okayama University) for fruitful discussion. This work was partially supported by a Grant-in-Aid of the Japanese Ministry of Education, Science, Sports and Culture (Grant Nos. 25400318 and 25400319).

References

[1] K. Sato, K. Numata, W. Dai, and M. Hunger: Appl. Phys. Lett. **104** (2014) 131901.
[2] K. Sato, K. Numata, W. Dai, and M. Hunger: Phys. Chem. Chem. Phys. **16** (2014) 10959.
[3] K. Sato, K. Fujimoto, K. Kawamura, W. Dai, and M. Hunger: J. Phys. Chem. C **116** (2012) 22954.
[4] K. Numata, K. Sato, and K. Fujimoto: Int. J. Nanosci. **11** (2012) 1240034.
[5] K. Sato, K. Fujimoto, W. Dai, and M. Hunger: J. Phys. Chem. C **117** (2013) 14075.
[6] K. Sato, K. Numata, and K. Fujimoto: Int. J. Nanosci. **11** (2012) 1240033.
[7] K. Sato and W. Sprengel: J. Chem. Phys. **137** (2012) 104906.
[8] S. J. Tao: J. Chem. Phys. **56** (1972) 5499.
[9] M. Eldrup, D. Lightbody, and J. N. Sherwood: Chem. Phys. **63** (1981) 51.
[10] K. Ito, T. Oka, Y. Kobayashi, Y. Shirai, K. Wada, M. Matsumoto, M. Fujinami, T. Hirade, Y. Honda, H. Hosomi, Y. Nagai, K. Inoue, H. Saito, K. Sakaki, K. Sato, A. Shimazu, and A. Uedono: Mater. Sci. Forum **607** (2009) 248.
[11] K. Ito, T. Oka, Y. Kobayashi, Y. Shirai, K. Wada, M. Matsumoto, M. Fujinami, T. Hirade, Y. Honda, H. Hosomi, Y. Nagai, K. Inoue, H. Saito, K. Sakaki, K. Sato, A. Shimazu, and A. Uedono: J. Appl. Phys. **104** (2008) 026102.
[12] P. Kirkegaard and M. Eldrup: Computer Phys. Commun. **7** (1974) 401.
[13] S. Morodome and K. Kawamura: Clays Clay Miner. **57** (2009) 150.
[14] H. Sato, A. Yamagishi, and K. Kawamura: J. Phys. Chem. B **105** (2001) 7990.